REPORT

Mutations in the *CEP290* (*NPHP6*) Gene Are a Frequent Cause of Leber Congenital Amaurosis

Anneke I. den Hollander,* Robert K. Koenekoop,* Suzanne Yzer, Irma Lopez, Maarten L. Arends, Krysta E. J. Voesenek, Marijke N. Zonneveld, Tim M. Strom, Thomas Meitinger, Han G. Brunner, Carel B. Hoyng, L. Ingeborgh van den Born, Klaus Rohrschneider, and Frans P. M. Cremers

Leber congenital amaurosis (LCA) is one of the main causes of childhood blindness. To date, mutations in eight genes have been described, which together account for ~45% of LCA cases. We localized the genetic defect in a consanguineous LCA-affected family from Quebec and identified a splice defect in a gene encoding a centrosomal protein (*CEP290*). The defect is caused by an intronic mutation (c.2991+1655A→G) that creates a strong splice-donor site and inserts a cryptic exon in the *CEP290* messenger RNA. This mutation was detected in 16 (21%) of 76 unrelated patients with LCA, either homozygously or in combination with a second deleterious mutation on the other allele. *CEP290* mutations therefore represent one of the most frequent causes of LCA identified so far.

Leber congenital amaurosis (LCA [MIM 204000]) is a severe retinal dystrophy, causing blindness or severe visual impairment at birth or during the first months of life. LCA is generally inherited in an autosomal recessive manner and is genetically heterogeneous. To date, mutations in eight genes (*AIPL1, CRB1, CRX, GUCY2D, IMPDH1, RDH12, RPE65,* and *RPGRIP1*) have been found to be associated with LCA.[1–3] Mutations in each of these genes have been identified in 2%–15% of patients with LCA, and, together, these eight genes account for ~45% of all LCA cases.[4–8]

We ascertained a consanguineous French Canadian family with four sibs affected by LCA (fig. 1*A*), and we excluded the involvement of all known LCA genes except *IMPDH1*. A genomewide linkage scan was performed to localize the causative gene defect. The four affected siblings were genotyped with 11,555 SNPs spread throughout the genome (Affymetrix GeneChip Human Mapping 10K Array). Multipoint linkage analysis was performed with Allegro[9] version 1.2c in the easyLINKAGE-Plus software package,[10] with use of the white allele frequencies. We identified four chromosomal intervals with multipoint LOD scores >2. All four regions were analyzed with polymorphic CA-repeat markers in the mother, the four affected sibs, and five unaffected sibs. Haplotype analysis excluded two of these regions. The highest multipoint LOD scores (2.9 and 3.0) were obtained at two chromosomal intervals: 12q21-q22 (*rs950017–rs1385060*) and 15q26 (*rs1384739–rs725213*). The region on chromosome 15 contained only one gene (*MCTP2*), which encoded a multiple C2-domain transmembrane protein. The coding exons and splice junctions were analyzed for mutations, but only known variants were detected.

The region on chromosome 12 contained 15 genes, including *CEP290* (or *NPHP6* [MIM 610142]) (fig. 1*A*). Mutations in this gene have recently been associated with pleiotropic forms of Joubert syndrome.[11,12] Joubert syndrome is an autosomal recessive disorder characterized by neurological features, including psychomotor delay, hypotonia, and ataxia. A typical neuroradiological feature of Joubert syndrome is the "molar tooth sign," indicating hypoplasia or aplasia of the cerebellar vermis. In addition to neurological features, patients with Joubert syndrome can develop nephronophthisis and retinal dystrophy. The clinical spectrum of Joubert syndrome associated with *CEP290* mutations is broad. Neurological symptoms typical of Joubert syndrome are present in all patients, but renal disease is either severe or absent. All analyzed patients have congenital amaurosis or retinitis pigmentosa. Nearly all patients carry nonsense or frameshift mutations on both alleles. An in-frame deletion in the *Cep290* gene was also recently associated with early-onset retinal degeneration in the *rd16* mouse.[13] After extensive evaluation, no gross brain or kidney pathology could be detected in these mice. CEP290 localizes to the centrosomes of dividing cells and to the connecting cilium of photoreceptors. CEP290 associates with several microtubule-based transport proteins, including RPGR, a protein that is mutated in patients with X-linked retinitis pigmentosa and cone-rod dystrophy.

From the Departments of Human Genetics (A.I.d.H.; S.Y.; M.L.A.; K.E.J.V.; M.N.Z.; H.G.B.; F.P.M.C.) and Ophthalmology (C.B.H.) and Nijmegen Centre for Molecular Life Sciences (A.I.d.H.; F.P.M.C.), Radboud University Nijmegen Medical Centre, Nijmegen, The Netherlands; McGill Ocular Genetics Centre, McGill University Health Centre, Montreal (R.K.K.; I.L.); The Rotterdam Eye Hospital, Rotterdam, The Netherlands (S.Y.; L.I.v.d.B.); Institute of Human Genetics, German Science Foundation National Research Center for Environment and Health, Munich-Neuherberg, Germany (T.M.S.; T.M.); Institute of Human Genetics, Technical University, Munich (T.M.S.; T.M.); and Department of Ophthalmology, University of Heidelberg, Heidelberg, Germany (K.R.)

Received May 20, 2006; accepted for publication June 28, 2006; electronically published July 11, 2006.

Address for correspondence and reprints: Dr. Anneke I. den Hollander, Department of Human Genetics, Radboud University Nijmegen Medical Centre, P.O. Box 9101, 6500 HB Nijmegen, The Netherlands. E-mail: a.denhollander@antrg.umcn.nl

* These two authors contributed equally to this work.

Am. J. Hum. Genet. 2006;79:556–561. 0002-9297/2006/7903-0019$15.00

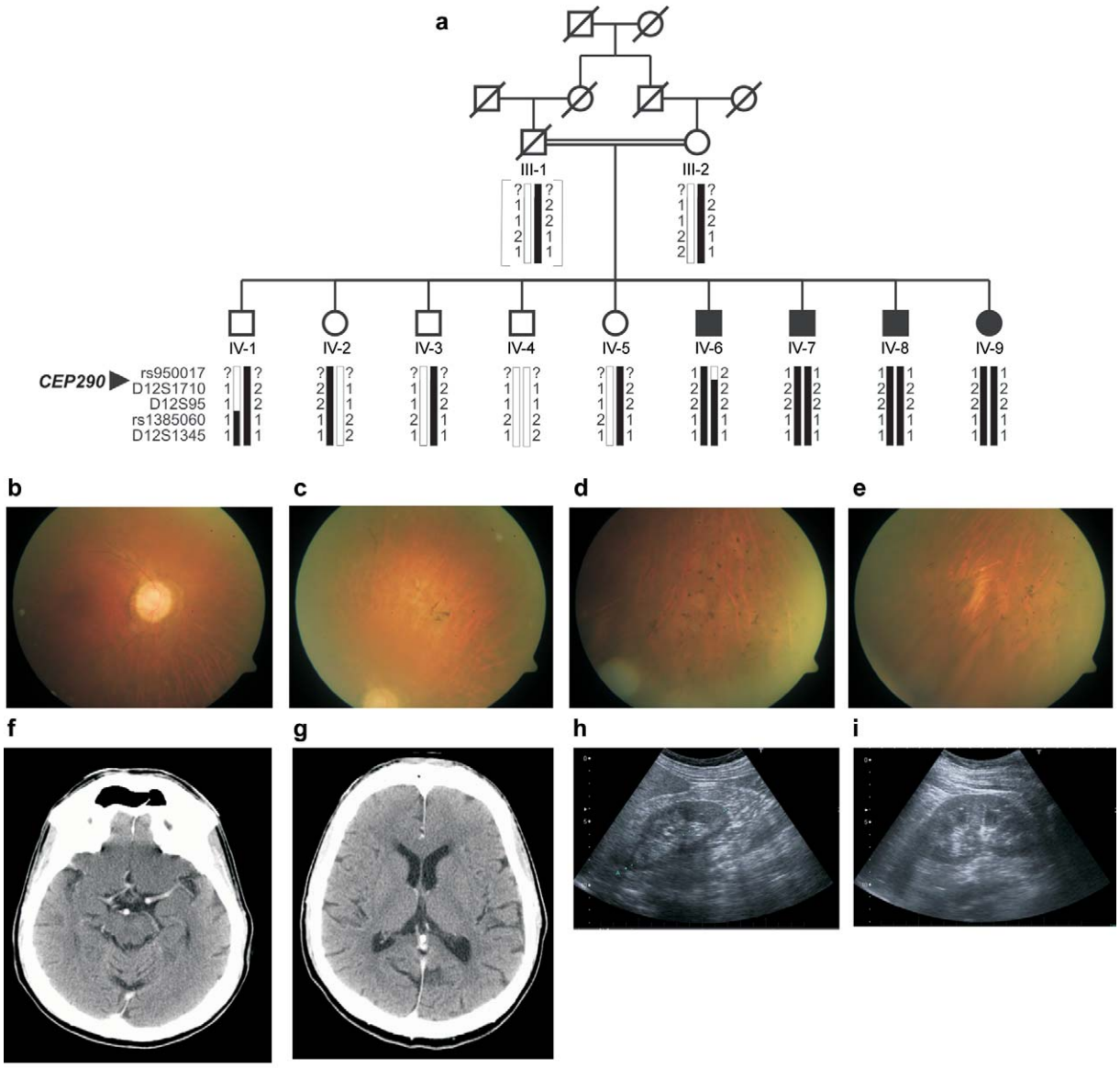

Figure 1. Pedigree and clinical features of the French Canadian LCA-affected family. *A,* Pedigree of the family. Four siblings are affected with LCA (*blackened symbols*), and the parents are first cousins. Haplotypes are shown for the chromosome 12 interval containing *CEP290*. *B–E,* Color fundus photographs of the right eye of affected sib IV-8 at age 45 years. *B,* Posterior pole, showing myopic changes, choroidal show, mild optic disc pallor, very significant arteriolar and venular narrowing, a poorly developed fovea, and peri-papillary atrophy, which extends along the superior arcade. *C,* Superior retina, showing a small isolated area of pigmentation, one bone spicule, and diffuse choroidal show. *D,* Inferior retina, showing small clumps of round pigmentation. *E,* Inferotemporal retina, showing more extensive small, round intraretinal pigmentation (nummular pigmentation). Images are slightly blurred because of a mild nuclear cataract. *F,* CT scan at the level of the midbrain of proband IV-7 at age 40 years. The axial view of the brain shows the normal structures of the midbrain and the cerebellum, without the molar tooth sign. *G,* CT scan of proband IV-7 at age 40 years at the level of the basal ganglia and the ventricles, depicting normal brain architecture, with no cerebellar atrophy. *H* and *I,* Kidney ultrasounds of affected sibling IV-6 at age 51 years. At the level of the parenchyma, both kidneys show isolated tiny foci of marked increased echogenicity, but without definite posterior shadowing. These are located mostly on the left side at the level of the cortex, but a few are also identified near the medulla on both sides and may indicate the presence of nephrocalcinosis. On both images, there are neither definite cysts nor dilatation of the collecting system or ureteral dilatation. There is no evidence of nephronophthisis.

The affected individuals of the French Canadian LCA-affected family were all blind or severely visually impaired at birth and showed wandering nystagmus since age ~6 wk. Patient IV-7 was first seen by us when he was age 43 years, and we observed that he had light-perception vision, with the oculodigital sign and enophthalmos. We also noted mild microphthalmia, a hyperopic refraction, marked keratoconus, dense white cataracts, ectopia lentis, and a pigmentary retinal degeneration with nummular pigmentations. Visual function was remarkably variable in the four affected sibs, ranging from light perception in patients IV-6 and IV-7 to more functional vision (20/150 acuities) in patient IV-8 and tunnel vision (30°) with 20/80 acuities in patient IV-9. The retinal aspect of patient IV-8, who has a myopic astigmatic refraction, is shown in figure 1*B*–1*E*. Two of the four affected sibs (IV-6 and IV-7) experienced seizures, which is not typical for Joubert syndrome, and had no other neurological symptoms. All four affected sibs had normal cognitive function. Detailed CT scanning (repeated five times) in patient IV-7 revealed no molar-tooth sign, no cerebellar atrophy, and no structural signs of Joubert syndrome (fig. 1*F* and 1*G*). The proband and the affected sibs are now in their 40s and 50s and have never exhibited any clinical signs of renal disease. Patient IV-6 had normal kidneys on renal ultrasound at age 51 years (fig. 1*H* and 1*I*).

Because of its function and the phenotype of *rd16* mice, we considered *CEP290* to be an excellent candidate gene for LCA in this French Canadian family. We sequenced all 53 coding exons and splice junctions and detected only one synonymous sequence variant (c.2055T→C [p.A685A]) in exon 21, which was not a known SNP. Since the variant is located between the splice-donor site and a predicted exonic splice enhancer (RESCUE-ESE[14]), we reasoned that it may have an effect on the splicing of this exon. However, RT-PCR performed on RNA isolated from an Epstein-Barr virus–immortalized lymphoblastoid cell line of patient IV-6 did not reveal aberrant splicing of exon 21. Subsequently, we analyzed the complete *CEP290* mRNA by RT-PCR, using 21 overlapping primer sets. An aberrant splice product was detected with a primer set

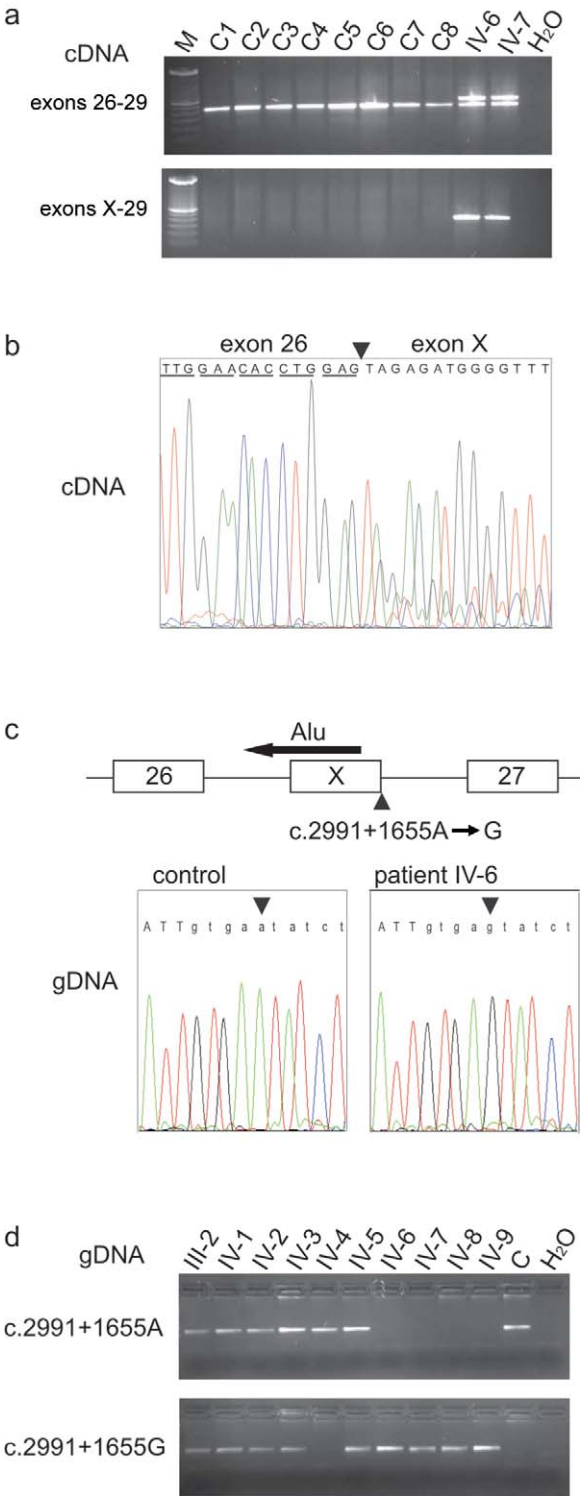

Figure 2. Molecular characterization of the *CEP290* mutation in the consanguineous LCA-affected family. *A,* Reverse transcription of *CEP290* mRNA and subsequent PCR using primers situated in exons 26–29 in two affected family members (IV-6 and IV-7), revealing a fragment of normal size and a larger aberrant fragment (*upper panel*). The aberrant fragment was not present in eight control individuals (C1–C8). RT-PCR using primers situated in the cryptic exon (X) and in exon 29 revealed an aberrant fragment in the patients with LCA but not in the controls (*lower panel*). Lane M contains a 100-bp marker. *B,* Sequencing of the aberrant RT-PCR product, showing that a cryptic exon (X) is spliced in between exons 26 and 27. The cryptic exon introduces a premature stop codon immediately downstream of exon 26. *C,* Cryptic exon X located 1.5 kb downstream of exon 26. Sequencing of the genomic DNA (gDNA) surrounding exon X revealed a mutation 5 bp downstream of the cryptic exon (c.2991+1655A→G). The mutation introduces a strong splice-donor site. Nucleotides in the cryptic exon are in uppercase letters, and intronic sequences are in lowercase letters. *D,* Allele-specific PCR showed that the c.2991+1655A→G mutation segregates with the disease in the family. All affected family members (IV-6, IV-7, IV-8, and IV-9) are homozygous for the mutation, whereas unaffected individuals are heterozygous or do not carry the mutation. Lane C represents a control individual.

Table 1. *CEP290* Mutations in Patients with LCA

		Allele 1		Allele 2	
Patient	Country	Mutation	Effect	Mutation	Effect
12832	Netherlands	c.2991+1655A→G	p.Cys998X	c.2991+1655A→G	p.Cys998X
13168	Germany	c.2991+1655A→G	p.Cys998X	c.2249T→G	p.Leu750X
14964	Germany	c.2991+1655A→G	p.Cys998X	c.7341dupA	p.Leu2448ThrfsX7
15103	Germany	c.2991+1655A→G	p.Cys998X	c.2118_2122dupTCAGC	p.Thr709SerfsX8
15212	Germany	c.2991+1655A→G	p.Cys998X	c.5866G→T	p.Glu1956X
16317	Netherlands	c.2991+1655A→G	p.Cys998X	c.2991+1655A→G	p.Cys998X
17971	Netherlands	c.2991+1655A→G	p.Cys998X	c.3814C→T	p.Arg1272X
20152	Netherlands	c.2991+1655A→G	p.Cys998X	c.679_680delGA	p.Glu227SerfsX1
21365	Netherlands	c.2991+1655A→G	p.Cys998X	c.2991+1655A→G	p.Cys998X
21393	Netherlands	c.2991+1655A→G	p.Cys998X	c.265dupA	p.Thr89AsnfsX1
21918	Netherlands	c.2991+1655A→G	p.Cys998X	c.180+1G→T	Splice defect
27228	Canada	c.2991+1655A→G	p.Cys998X	c.2991+1655A→G	p.Cys998X
27242	Canada	c.2991+1655A→G	p.Cys998X	c.1550delT	p.Leu517X
27245	Canada	c.2991+1655A→G	p.Cys998X	c.4115_4116delTA	p.Ile1372LysfsX4
27246	Canada	c.2991+1655A→G	p.Cys998X	c.4966G→T	p.Glu1656X
27250	Italy	c.2991+1655A→G	p.Cys998X	c.5813_5817delCTTTA	p.Thr1938AsnfsX15

designed to amplify exons 26–29 (fig. 2*A*). Sequencing of the product revealed the insertion of a 128-bp cryptic exon between exons 26 and 27, which introduces a stop codon immediately downstream of exon 26 (fig. 2*B*). Notably, a small amount of wild-type product is still present in the affected individuals. The aberrant splice product was not detected in eight control individuals (fig. 2*A*).

The sequence of the cryptic exon is located in intron 26, 1.5 kb downstream of exon 26, and contains part of an *Alu* element. In the wild-type sequence, the exon is preceded by a strong splice-acceptor site (splice prediction score 0.93), but no splice-donor site is predicted (NNSPLICE version 0.9; BDGP Splice Site Prediction by Neural Network Web site).[15] We sequenced the genomic DNA surrounding the cryptic exon in patient IV-6 and detected an A→G transition 5 bp downstream of the cryptic exon (c.2991+1655A→G) (fig. 2*C*). The mutation creates a strong splice-donor site (splice prediction score 0.90), which presumably leads to efficient splicing of the cryptic exon into the *CEP290* mRNA. The mutation segregates with the disease in the family (fig. 2*D*).

To determine whether this mutation could be a common cause of LCA, we screened 76 unrelated patients with LCA for the c.2991+1655A→G mutation by allele-specific PCR.[16] The involvement of known LCA genes was previously excluded in these patients by microarray-based mutation detection[6] and/or comprehensive heteroduplex analysis. Strikingly, 4 patients were homozygous for the mutation, and 12 were heterozygous for c.2991+1655A→G (table 1). The mutation was not detected in 223 French Canadian controls, and 1 of 248 Dutch control individuals was found to be heterozygous for the mutation.

These results indicate that the c.2991+1655A→G mutation is an important cause of LCA and may explain up

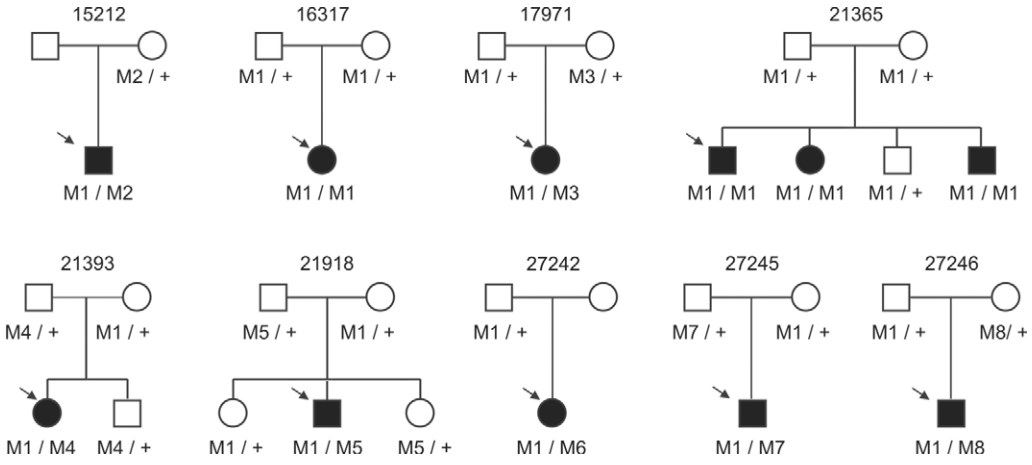

Figure 3. Segregation analysis of *CEP290* mutations in nine LCA-affected families. In all nine families, segregation of the mutations is in agreement with autosomal recessive inheritance. For each family, the proband is indicated (*arrow*). M1 = c.2991+1655A→G; M2 = p.Glu1956X; M3 = p.Arg1272X; M4 = p.Thr89AsnfsX1; M5 = c.180+1G→T; M6 = p.Leu517X; M7 = p.Ile1372LysfsX3; M8 = p.Glu1656X; + = wild type.

to 21% of LCA cases. Under the assumptions of an overall incidence of LCA of 1/100,000 individuals in the white population and the involvement of *CEP290* mutations in 10% of patients with LCA, the Hardy-Weinberg equation predicts a total *CEP290* mutant allele frequency of 1/1,000 and a carrier frequency of 1/500 individuals. Under the assumption that the c.2991+1655A→G variant constitutes two-thirds of all mutant alleles, a carrier frequency of 1/750 individuals is predicted. If *CEP290* variants underlie 30% of LCA cases, a carrier frequency of 1/433 individuals is predicted.

The 12 patients who were heterozygous for c.2991+1655A→G were analyzed for additional mutations in the 53 coding exons and splice junctions of *CEP290* by heteroduplex analysis and/or direct sequencing. In all patients, we detected a heterozygous mutation on the other allele (table 1). Five mutations introduce a premature stop codon, six lead to a frameshift, and one affects the invariable GT dinucleotide of the splice-donor site of exon 3.

In nine families in which two *CEP290* mutations were identified, family members were available for segregation analysis. In all nine families, segregation of the variants as expected for autosomal recessive inheritance was observed (fig. 3). Patients had no neurological symptoms typical of Joubert syndrome, had normal cognitive function, and showed no clinical signs of renal disease. Patient 21393 had abnormal proprioception but was otherwise healthy. Clinical details of four representative patients are given below.

Patient 27245 is a male baby who was first seen by us when he was age 10 mo. His head circumference was found to be large by a pediatrician, and he underwent magnetic resonance imaging and ultrasound of the brain, which were found to be normal by a pediatric neuroradiologist. Ultrasound studies of both kidneys also had normal findings. On ophthalmic evaluation, we found that the child had no fixation and did not follow a near target. He exhibited the oculodigital sign, and refractions revealed a marked hyperopia. Retinal examination showed narrow vessels, mottled retinal pigment epithelium, and multiple white intraretinal dots. Electroretinogram (ERG) testing revealed nondetectable rod and cone responses.

Patient 27242 also had a completely normal brain CT. On eye examination at age 7 mo, no visual behavior was seen, and there was no fixation and no following of a target. She exhibited the oculodigital sign, nystagmus, and high hyperopia. The retinal appearance was essentially normal, with mild vascular attenuation. The ERG signals were nondetectable.

At age 18 mo, patient 27246 did not exhibit visual behavior and had wandering nystagmus, the oculodigital sign, high hyperopia, and nondetectable ERG signals. The retinal appearance was essentially normal. Patient 27250 was also blind at birth, with light-perception vision, and we documented posterior pole cataracts, keratoconus, and nondetectable ERG signals.

The *CEP290* c.2991+1655A→G mutation was detected in 16 (21%) of 76 unrelated patients with LCA and thus represents one of the most frequent causes of LCA identified so far. Patients carrying this mutation originate from various geographic regions, including Canada, Germany, The Netherlands, and Italy. The mutation leads to aberrant splicing, but a small amount of correctly spliced product is still present, which suggests that this may be sufficient for normal cerebellar and renal function but not for correct function of the photoreceptors. Complete loss of function of both *CEP290* alleles leads to Joubert syndrome, whereas patients with LCA have a small amount of residual *CEP290* activity. This dosage-dependent mechanism is similar to earlier findings for the *ABCA4* gene, implicated in Stargardt disease, cone-rod dystrophy, and retinitis pigmentosa, and for the *USH2A* gene, which has been associated with nonsyndromic retinitis pigmentosa and Usher syndrome.[17,18]

Acknowledgments

We thank Dr. A. de Brouwer and Dr. R. Roepman, for their helpful discussions, and C. Beumer and S. van der Velde-Visser, for excellent technical assistance. We thank all the LCA families involved and C. Robert and R. Pigeon for coordinating the visits. We are indebted to Dr. L. Carpineta, a pediatric neuroradiologist, for critically evaluating the brain CT scans and the renal ultrasounds of the proband and the affected sibling. We thank photographer C. Riopel, for the retinal photos, and Drs. I. van den Burgt and H. Kroes, for consulting on the patients. This work was supported by the Netherlands Organisation for Scientific Research (grant 916.56.160 [to A.I.d.H.]), the British Retinitis Pigmentosa Society (grant GR543 [to A.I.d.H. and F.P.M.C.]), Stichting Wetenschappelijk Onderzoek Oogziekenhuis (to L.I.v.d.B., A.I.d.H., and F.P.M.C.), the Foundation Fighting Blindness Canada (to R.K.K. and F.P.M.C.), and the Fonds de la Recherche en Santé Québec (to R.K.K.).

Web Resources

The URLs for data presented herein are as follows:

BDGP Splice Site Prediction by Neural Network, http://www.fruitfly.org/seq_tools/splice.html (for NNSPLICE version 0.9)
Online Mendelian Inheritance in Man (OMIM), http://www.ncbi.nlm.nih.gov/Omim/ (for LCA and *CEP290*)
RESCUE-ESE, http://genes.mit.edu/burgelab/rescue-ese/ (for prediction of exonic splice enhancers)

References

1. Cremers FPM, van den Hurk JAJM, den Hollander AI (2002) Molecular genetics of Leber congenital amaurosis. Hum Mol Genet 11:1169–1176
2. Janecke AR, Thompson DA, Utermann G, Becker C, Hübner CA, Schmid E, McHenry CL, Nair AR, Rüschendorf F, Heckenlively J, Wissinger B, Nürnberg P, Gal A (2004) Mutations in *RDH12* encoding a photoreceptor cell retinol dehydrogenase cause childhood-onset severe retinal dystrophy. Nat Genet 36:850–854
3. Bowne SJ, Sullivan LS, Mortimer SE, Hedstrom L, Zhu J, Spellicy CJ, Gire AI, Hughbanks-Wheaton D, Birch DG, Lewis RA,

Heckenlively JR, Daiger SP (2006) Spectrum and frequency of mutations in IMPDH1 associated with autosomal dominant retinitis pigmentosa and Leber congenital amaurosis. Invest Ophthalmol Vis Sci 47:34–42

4. Hanein S, Perrault I, Gerber S, Tanguy G, Barbet F, Ducroq D, Calvas P, Dollfus H, Hamel C, Lopponen T, Munier F, Santos L, Shalev S, Zafeiriou D, Dufier J-L, Munnich A, Rozet J-M, Kaplan J (2004) Leber congenital amaurosis: comprehensive survey of the genetic heterogeneity, refinement of the clinical definition, and genotype-phenotype correlations as a strategy for molecular diagnosis. Hum Mutat 23:306–317
5. Zernant J, Kulm M, Dharmaraj S, den Hollander AI, Perrault I, Preising MN, Lorenz B, Kaplan J, Cremers FPM, Maumenee I, Koenekoop RK, Allikmets R (2005) Genotyping microarray (disease chip) for Leber congenital amaurosis: detection of modifier alleles. Invest Ophthalmol Vis Sci 46:3052–3059
6. Yzer S, Leroy BP, De Baere E, de Ravel TJ, Zonneveld MN, Voesenek K, Kellner U, Martinez Ciriano JP, de Faber J-THN, Rohrschneider K, Roepman R, den Hollander AI, Cruysberg JR, Meire F, Casteels I, van Moll-Ramirez NG, Allikmets R, van den Born LI, Cremers FPM (2006) Microarray-based mutation detection and phenotypic characterization of patients with Leber congenital amaurosis. Invest Ophthalmol Vis Sci 47: 1167–1176
7. Dharmaraj SR, Silva ER, Pina AL, Li YY, Yang JM, Carter CR, Loyer MK, El Hilali HK, Traboulsi EK, Sundin OK, Zhu DK, Koenekoop RK, Maumenee IH (2000) Mutational analysis and clinical correlation in Leber congenital amaurosis. Ophthalmic Genet 21:135–150
8. Lotery AJ, Namperumalsamy P, Jacobson SG, Weleber RG, Fishman GA, Musarella MA, Hoyt CS, Héon E, Levin A, Jan J, Lam B, Carr RE, Franklin A, Radha S, Andorf JL, Sheffield VC, Stone EM (2000) Mutation analysis of 3 genes in patients with Leber congenital amaurosis. Arch Ophthalmol 118:538–543
9. Gudbjartsson DF, Jonasson K, Frigge ML, Kong A (2000) Allegro, a new computer program for multipoint linkage analysis. Nat Genet 25:12–13
10. Hoffmann K, Lindner TH (2005) easyLINKAGE-Plus: automated linkage analyses using large-scale SNP data. Bioinformatics 21:3565–3567
11. Sayer JA, Otto EA, O'toole JF, Nurnberg G, Kennedy MA, Becker C, Hennies HC, et al (2006) The centrosomal protein nephrocystin-6 is mutated in Joubert syndrome and activates transcription factor ATF4. Nat Genet 38:674–681
12. Valente EM, Silhavy JL, Brancati F, Barrano G, Krishnaswami SR, Castori M, Lancaster MA, Boltshauser E, Boccone L, Al-Gazali L, Fazzi E, Signorini S, Louie CM, Bellacchio E, International Joubert Syndrome Related Disorders Study Group, Bertini E, Dallapiccola B, Gleeson JG (2006) Mutations in *CEP290,* which encodes a centrosomal protein, cause pleiotropic forms of Joubert syndrome. Nat Genet 38:623–625
13. Chang B, Khanna H, Hawes N, Jimeno D, He S, Lillo C, Parapuram SK, Cheng H, Scott A, Hurd RE, Sayer JA, Otto EA, Attanasio M, O'toole JF, Jin G, Shou C, Hildebrandt F, Williams DS, Heckenlively JR, Swaroop A (2006) In-frame deletion in a novel centrosomal/ciliary protein CEP290/NPHP6 perturbs its interaction with RPGR and results in early-onset retinal degeneration in the *rd16* mouse. Hum Mol Genet 15: 1847–1857
14. Fairbrother WG, Yeh RF, Sharp PA, Burge CB (2002) Predictive identification of exonic splicing enhancers in human genes. Science 297:1007–1013
15. Reese MG, Eeckman FH, Kulp D, Haussler D (1997) Improved splice site detection in Genie. J Comput Biol 4:311–323
16. Little S (2000) Amplification-refractory mutation system (ARMS) analysis of point mutations. In: Boyle AL (ed) Current protocols in human genetics. John Wiley & Sons, New York, pp 9.8.1–9.8.12
17. Cremers FPM, van de Pol TJR, van Driel M, den Hollander AI, van Haren FJJ, Knoers NVAM, Tijmes N, Bergen AAB, Rohrschneider K, Blankenagel A, Pinckers AJLG, Deutman AF, Hoyng CB (1998) Autosomal recessive retinitis pigmentosa and cone-rod dystrophy caused by splice site mutations in the Stargardt's disease gene *ABCR*. Hum Mol Genet 7:355–362
18. Rivolta C, Sweklo EA, Berson EL, Dryja TP (2000) Missense mutation in the *USH2A* gene: association with recessive retinitis pigmentosa without hearing loss. Am J Hum Genet 66: 1975–1978